

Simple glass-forming liquids: their definition, fragilities, and landscape excitation profiles

This article has been downloaded from IOPscience. Please scroll down to see the full text article.

1999 J. Phys.: Condens. Matter 11 A75

(<http://iopscience.iop.org/0953-8984/11/10A/005>)

View [the table of contents for this issue](#), or go to the [journal homepage](#) for more

Download details:

IP Address: 129.252.86.83

The article was downloaded on 27/05/2010 at 11:25

Please note that [terms and conditions apply](#).

Simple glass-forming liquids: their definition, fragilities, and landscape excitation profiles

C A Angell, B E Richards and V Velikov

Department of Chemistry, Arizona State University, Tempe, AZ 85287, USA

Received 2 October 1998

Abstract. The ‘excitation profile’ of a liquid is a measure of the rate per kelvin at which the liquid is driven by entropy generation to the top of its potential energy landscape. We argue that it determines the liquid fragility, and hence controls the canonical features of viscous liquid phenomenology. We seek to prove this using studies of simple glass formers. We recognize two types of simple glass former, molecularly simple and excitationally simple, and provide examples and characterization of each.

In the first category we describe the systems S_2Cl_2 , CS_2 , and their binary solutions. The simplest case CS_2 is only glass forming in emulsion form but solutions in S_2Cl_2 up to 85% CS_2 are found to be bulk glass formers. The fragility of each component is determined by the new ‘reduced-transition-width’ measurement and found to be only 60% fragile versus 75% for the fragile liquid toluene and propylene carbonate. We infer that the mixed LJ (Lennard-Jones) system, whose landscape ‘excitation profile’ has recently been determined by MD computer simulations, is only a moderately fragile liquid. For S_2Cl_2 the increase in heat capacity at T_g is used to ‘quantify’ the energy landscape and establish the appropriate ‘excitation profile’ for liquids of this fragility.

The second type of simplicity is bestowed by the presence of a single dominant interaction in the system. The best cases are the covalent glass formers of the chalcogenide variety, e.g. Ge–Se, and Ge–As–Se, in which the breaking of angle-specific covalent bonds is the dominant excitation process. We show that in the ground-state bond lattice an extremum in the glass transition temperature occurs close to the theoretical rigidity percolation bond density of 2.4 bonds per particle where a fragility minimum is also found. Invoking a simple theoretical treatment of this bond lattice we find that the entropy of the elementary excitation is a minimum or zero at percolation, and the glass transition becomes a simple Schottky anomaly with kinetic arrest. The excitation profile predicted by this model seems similar to that found by the simulations for the molecularly simple glasses. The fragility of the liquid is, in this case, controlled by the entropy change in the elementary excitation process. Whether this excitation entropy is determined within the configurational or vibrational densities of states is a key question. In either case, large values mean sharp excitation profiles which, due to cooperative effects near pure Ge, can become first-order liquid–liquid transitions.

1. Introduction

In this paper we introduce two key notions related to understanding the ‘glassy-state’ problem. One is the notion of the ‘excitation profile’ for an amorphous system, and the other is the notion of the ‘simple glass former’. The attributes of the latter may be used, in quite different ways, to calculate and characterize the former. The excitation profile itself directly reflects the liquid fragility. Therefore, through the known correlations of fragility with non-exponentially and non-linearity, it controls the phenomenology of the glass-forming liquid, and of the glass that it forms.

The upper portion of what we are calling the excitation profile was presented recently [1] for a mixed LJ (Lennard-Jones) system as the energy of the ‘inherent structures’ versus the temperature at which the system had been equilibrated (prior to the quench procedure which identifies the potential energy of the inherent structure [2]). The *inherent-structure energy* is the potential energy of the structure to which the system has been driven by the TS term in the Helmholtz free energy $A = E - TS$ which the system must minimize in order to be in thermal equilibrium at the temperature T . The lower portion of the profile cannot be ‘seen’ by simulations because of the intervention of the glass transition for the simulated system. This occurs when the structural relaxation time for the temperature in question exceeds the computer time available for the study [3] (currently about 10 ns). A smaller portion of this same profile was presented for the case of a one-component LJ system more than a decade ago [4], when the available time was only about 10 ps. We can complete the excitation profile presented by Sastry *et al* using the value of T_c of the mode-coupling theory [5], obtained by Kob and Andersen [6] for the mixed LJ system, and the observation that T_c/T_K for systems of comparable character is ~ 1.6 (see below). This excitation profile is shown in figure 1.

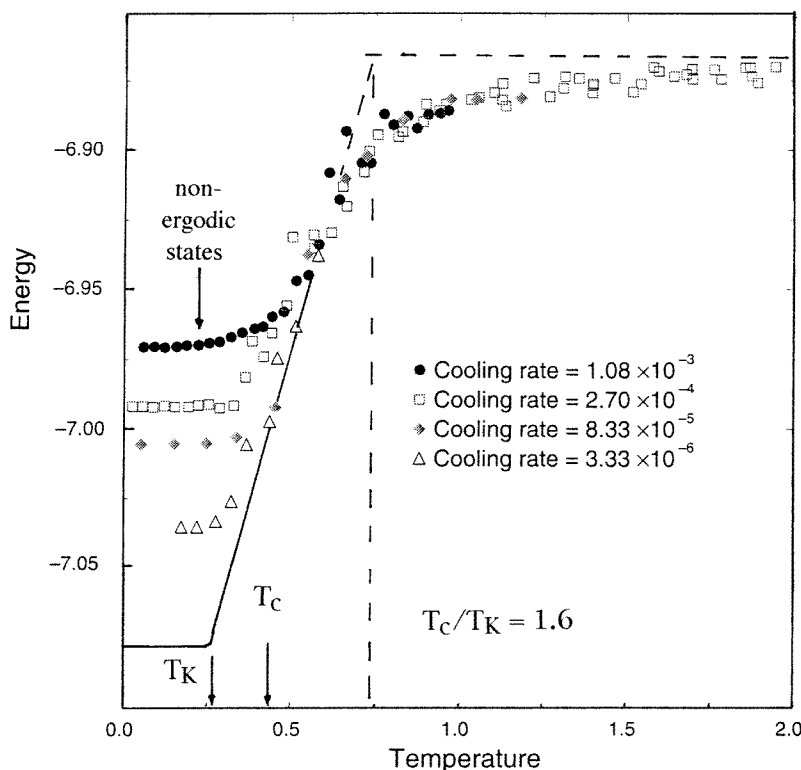


Figure 1. The configuron ‘excitation profile’ for a system of mixed LJ particles, based on the inherent structure versus energy determinations for this system obtained [1] from assessments using different cooling rates (see the key) and extrapolating to infinitely small cooling rates using the observation, based on data for moderately fragile liquids, that $T_c/T_K \sim 1.6$ [8]. (Adapted from reference [1], by permission.)

The profile of figure 1 shows a singularity on arrival at the ground state, as is usually envisaged in discussion of the Kauzmann temperature [7]. However, there is no need for this, as will be emphasized later. The temperature T_c occurs less than half-way to the ‘top of

the landscape', in contrast to the expectation expressed by one of us for fragile liquids [8]. Since it has always seemed natural to expect the simple mixed-atom liquids to be very fragile, this is a matter for concern. We will therefore first address the question of simple molecular glass-former behaviour to see whether the expectation of fragile behaviour for LJ and mixed LJ systems is a valid one.

2. Simple glass formers

In this paper we focus attention on two types of simple glass former—those that are simple by virtue of their molecular simplicity, and those that are simple by virtue of the dominance of a single type of interaction, particularly a covalent bond.

2.1. Molecularly simple glass formers

Simply constituted glass formers are uncommon because most simple molecules have little difficulty in finding an efficient packing which guarantees that melting at T_m will only occur when the product $T \Delta S$ needed to overcome the energetic advantage of the crystal over amorphous packing, ΔH , occurs when T is not far from the boiling point, T_b . The hot liquid is highly fluid, and crystallization on cooling below T_m occurs very readily. However, there are a few molecules which happen to have shapes and/or atomic-size relations for which no efficient packing exists, and then the melting condition is met when $T \ll T_b$. The melt is then viscous at T_m , crystal nucleation is slow, and crystal growth is inhibited, i.e. glasses form [9]. Empirically it is found that this is common if the system meets the condition $T_b/T_m = 2.0$. The three-atom molecule CS_2 is on the borderline of this criterion, $T_b/T_m = 1.97$, while the four-atom molecule S_2Cl_2 ($T_b/T_m = 2.09$) is a 'good' glass former. 15% of S_2Cl_2 in a $\text{CS}_2 + \text{S}_2\text{Cl}_2$ solution proves sufficient to permit vitrification of small samples [10].

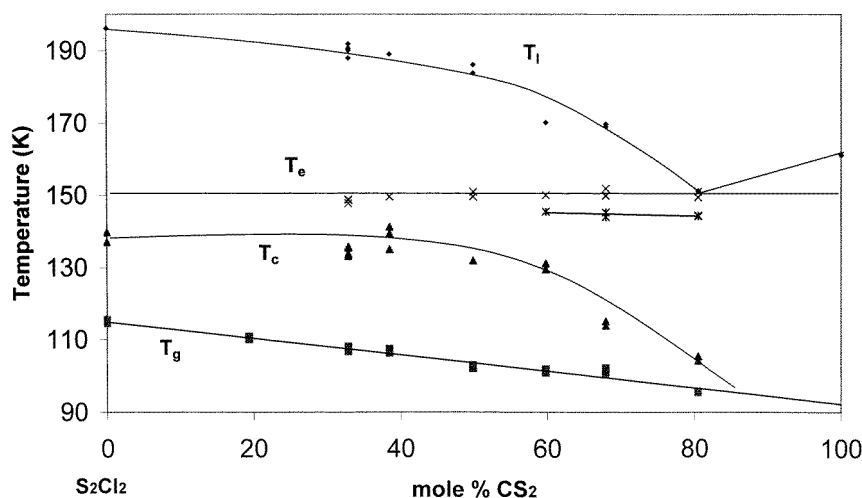


Figure 2. The glass-forming composition region and glass transition temperatures T_g for the molecularly simple system sulphur monochloride + carbon disulphide ($\text{S}_2\text{Cl}_2 + \text{CS}_2$). T_l is the liquidus temperature, T_e is the eutectic temperature and T_c is the crystallization temperature. Stability against crystallization maximizes near 50 mol% CS_2 . The system appears to be a simple eutectic, but the endothermic effects below the eutectic temperature are unexplained.

The glass transition temperatures for solutions in this system are shown in figure 2 which contains also the approximate phase diagram. The variation in T_g is linear, suggesting ideal solution behaviour. This contrasts with the behaviour in the system CS_2 + toluene [11] which shows strongly curvilinear behaviour over the same glass-forming solution range but still yields the same extrapolated T_g for pure CS_2 , 92 K.

The fragilities of the pure components CS_2 and S_2Cl_2 may now be estimated in either of two ways. Firstly the limited viscosity data available [12] may be compared with those for other liquids on a T_g -scaled basis [13, 14]—which gives only qualitative information but shows that both liquids are less fragile than, for instance, the well studied case of orthoterphenyl [13]. Secondly, the fragility can be obtained semi-quantitatively from the reduced width of the glass transition as demonstrated recently for molecular liquids [15], and as can be demonstrated for inorganic network liquids from correlation of the T_g -width with the viscosity activation energy proposed by Moynihan [16].

The cited measurements [15, 16] were made using differential scanning calorimetry studies and the full glass transition width. Because of S_2Cl_2 corrosivity problems, the present measurements were made in glass tubes using differential thermal analysis, and the transition widths are differently defined, as in figure 3. To deal with this difference we use the well known liquid toluene [14, 17] as a fragility calibration standard.

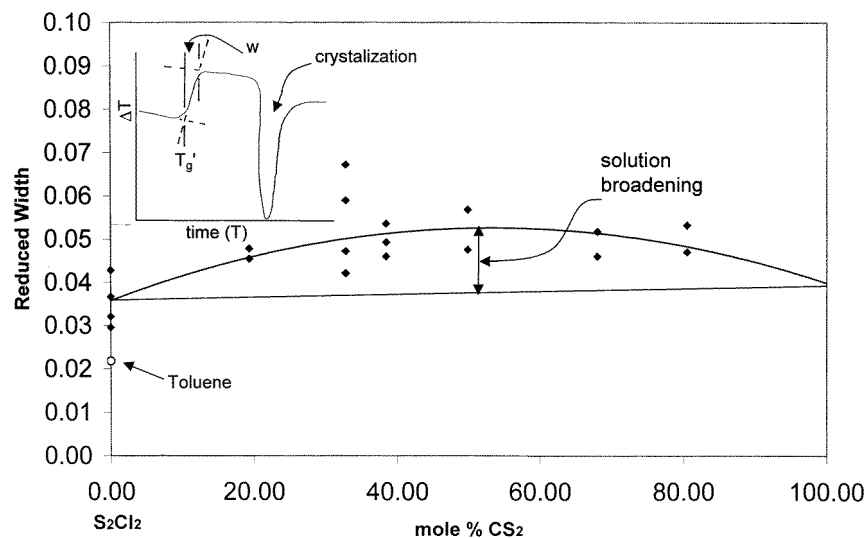


Figure 3. The reduced widths of the glass transitions w/T'_g in relation to the solution composition in the system S_2Cl_2 + CS_2 . A typical DTA scan through the glass transition up to crystallization, and the definition of the transition width, are shown in the inset. For fragility calibration, the width, measured with the present set-up for the well characterized liquid toluene, is shown on the left-hand axis. Strong liquids have transition widths near or above 0.10 on this scale.

The reduced transition widths for the binary S_2Cl_2 + CS_2 system are shown in figure 3. They are seen to be the same for the two end members, each of which has a width almost twice that of toluene. Note the presence of a symmetrical broadening of the transitions with solution composition which reaches a maximum at 50 mol%. We assign this to the effect of a distribution of environments with different values of T_g , rather than to any decrease of fragility with mixing, and will discuss it in a later paper [10].

Scaling the end-member widths to the fragility $F_{1/2}$ -scale using the value for toluene

$F_{1/2} = 0.73$ (or 73% fragile) we obtain the value of $F_{1/2}(\text{CS}_2 \text{ and } \text{S}_2\text{Cl}_2) = 0.57$ or 57% fragile. This value is comparable to that of bromobutane, 0.59 (59% fragile) [18, 19], and considerably below the values for common fragile glass formers: orthoterphenyl (oTP): 0.71; propylene carbonate (pc): 0.74; and $[\text{Ca}(\text{NO}_3)_2]_{40} [\text{KNO}_3]_{60}$ (CKN): 0.75.

To the extent that the molecules CS_2 and S_2Cl_2 approach the LJ system in simplicity, it would then seem that LJ and mixed LJ systems should behave as moderately fragile liquids only. That it is reasonable to compare the two can be supported by the measured change in heat capacity of S_2Cl_2 at T_g with that of a mixed LJ system on a per-heavy-atom basis. For S_2Cl_2 the number is $18 \text{ J K}^{-1} \text{ mol}^{-1}$ of atoms [20], while for LJ argon and mixed LJ systems, measured at a temperature higher than the ‘normal’ T_g , the value of ΔC_p is $16.5 \text{ J K}^{-1} \text{ mol}^{-1}$ of atoms [6]. In each case the heat capacity of the glass is classical ($3R$ per gram atom) at T_g (the latter case of necessity, since the model is classical).

Elsewhere [8] this heat capacity has been used, together with the assumption that there are $e^{\alpha N}$ ($\alpha \sim 1$) states per mole of heavy particles [21], to argue that the landscape entropy is fully excited by a temperature of $1.56 T_K$ or somewhat above the mode-coupling critical temperature T_c for fragile liquids. (T_c is also the dynamic crossover temperature identified by the scaling procedures of Rössler and Sokolov [22], the Stickel temperature identified by derivative data analysis by Stickel *et al* [23] and the α - β bifurcation temperature.) Since for a bromobutane-like molecule, $1.56/T_K$ would be close to the T_c -value, it would seem from figure 1 that this estimate cannot be correct. The total entropy needs to be higher or the heat capacity smaller. The temperature characteristic of the top of the landscape $T_{ToL} = E_{ToL}/k_B$ is a strong function of the landscape entropy, so the number of states need only exceed $e^{\alpha N}$ by a small amount, e.g. with $\alpha \sim 1.5$, which is within the estimates. Likewise, assignment of a part of the observed heat capacity jump to non-configurational origins (e.g. decrease in vibration frequencies as seems likely, see section 2.2.4) would push T_{ToL} to higher values.

An important result of this line of thought, though, is that the larger the value of ΔC_p the more rapidly the entropy increases with temperature, so the more rapidly the state point will be ‘floated’ to the top of the landscape. Thus the fragile liquids, which are those with higher heat capacities per mole of heavy atoms, have steeper excitation profiles. The corresponding density of states, which is the gradient of the excitation profile, will be narrow in energy. The same result follows from the considerations of the next section, in which the steepness of the profile, i.e. the fragility, will be seen to be determined by a single excitation parameter.

2.2. Excitationally simple glass formers

In this section we deal with systems for which it is reasonable to assume that most of the thermodynamics, and hence the main features of the dynamics [1], are determined by the breaking of well defined bonds. Then it is possible to transpose from the strongly interacting elements of the particle lattice to the weakly interacting elements of the ‘bond lattice’, and in a first approximation to treat the bonds as independently excitable [24]. In a case like that of the Se-rich Ge–Se alloys that we consider here, the two bonds which are of relevance are of almost equal bond strengths, so a very simple treatment of the system thermodynamics may be executed.

We will first briefly examine two aspects of this system’s behaviour. The first concerns the relevance of the concept of ‘rigidity percolation’ [25], which is expected to lead to extremes of behaviour near a ‘bond density’ of 2.4 bonds per particle (on average) [25, 26]. This will prove to be associated with an extreme value in one of the two bond excitation parameters. Then we will consider the use of the ‘bond model’ in characterizing, by the direct calculation route, the full excitation profile. This profile is determined by the same excitation parameter whose

composition dependence is found to be responsible for the hiding of the rigidity percolation singularity in real glasses. This phenomenon is present (at the predicted bond density) in the ground state of the system, as we will demonstrate below.

2.2.1. Rigidity percolation. One of the earliest applications of the Maxwell concept of constraint counting to the field of materials science was that of Phillips [26] who was interested in the reasons that certain liquid chalcogenide systems are kinetically very stable against crystallization [27]. Phillips concluded that stability of the glass would be maximized when the *bond density* (the number of bonded neighbours per atom in the structure) averaged 2.4.

Subsequent theoretical [25, 28, 29] and experimental [30–38] applications of the concept in this area were more concerned with the description of the physical properties of these glassy materials, in particular with respect to behaviour in the vicinity of the composition at which the constraints and degrees of freedom equalize. The constraints are evaluated at the molecular level in terms of the fixed bond lengths and bond angles, and it is predicted that the equalization condition is met when the bond density, usually called the average coordination number and designated $\langle r \rangle$, is equal to 2.4. (Here ‘coordination number’ must be understood in the restricted sense of the coordination of each atom with respect to *bonded* neighbours only, which is why we introduce the less ambiguous term.) In binary and multicomponent systems, the bond density can be varied continuously by varying the content of elements with different bonding propensities, e.g. 2 for chalcogenide elements S, Se and often Te, 3 for pnictides P, As, Sb, and often Bi, and 4 for Si, Ge, and often Sn.

Properties, like the glass transition temperature and the heat capacity jump at T_g , have been studied for a number of different multicomponent systems [27, 31–38], and breaks of one sort or another have been observed in the vicinity of the ‘rigidity percolation threshold’ [29], the name assigned to the theoretical transition at $\langle r \rangle = 2.4$ where floppy regions become isolated within a continuous rigid matrix. However, the relation of these breaks to the theoretical expectations needs to be looked at carefully.

The theoretical treatments of rigidity percolation in glassy systems have always been concerned with idealized structures in which all possible bonds are intact and all bond-angle rules respected. The reason that liquids form from glasses on heating is that a fraction of these constraints, which is a Boltzmann function of temperature, are lifted. The state of excitation is most sensitively monitored by the structural relaxation time, which determines the liquid viscosity η through the Maxwell equation connecting it to the shear modulus measured at high frequency G_∞ and the shear relaxation time τ :

$$\eta = G_\infty \tau. \quad (1)$$

G_∞ , which measures shear rigidity, depends linearly on temperature via the broken constraint fraction and τ depends on it more strongly, indeed exponentially, as will be discussed further below. Inversely, on cooling, the constraints tend to be re-established. However, a fraction remain broken, i.e. are frozen in, when the relaxation time reaches the value at which the equilibrium state can no longer be maintained for the cooling rate in question. (We say that ‘ergodicity is broken’.) This means that in the real glasses used to test the predictions of the models, the fraction of constraints acting on the system of atoms cannot be the number calculated from the composition. Therefore the effects predicted by the theory cannot be expected to occur at the theoretical percolation threshold. So far this problem has not been mentioned in attempts [28, 29] to explain the observations that the observed increases in rigidity with increasing bond density occur at values higher than the simple theory predicts [34, 35, 37].

Recently [39], we tried to put this ‘broken-constraint’ factor into the picture, and we reproduce the findings here. We use data for the cases of the three-component chalcogenide

glass system Ge–As–Se for which data are available in convenient form for our analysis [31]. Comparable information is available for other systems [32–38]. It turns out that the effect of the fraction of constraints that are frozen in on properties like the glass transition temperature is largest *just* in the vicinity of the transition that is anticipated by the theory. A later subsidiary purpose will be to relate these effects to the ‘energy landscape’ approach to the discussion of liquid properties [2, 40], which has been repeatedly invoked in the discussion of glasses [41] and more recently has been shown to be intimately related to the details of the relaxation function [1] and also to the fragility of the liquid [8, 42].

The effect of allowing for the effect of frozen-in constraints on the relation of the glass transition versus $\langle r \rangle$ will be evaluated from previously published information on liquids and glasses for the system Ge–As–Se [31, 36], and data for the liquid states of these systems will then be used to parameterize a simple but relevant treatment of the effect of temperature on the thermodynamic and relaxational behaviour of these systems. These results, and the parameters which control them, will then be shown to contain a description of the excitation profile, previously obtained only from configuration-space analysis for other systems.

2.2.2. Ideal glass transitions for the Ge–As–Se system. The state of the liquid system from which no further entropy can be lost by configurational rearrangements is known as an *ideal glass* [43]. All other glasses are, in principle, isothermally rearrangeable into this ideal state with a decrease in probability, and hence in free energy. It is only a matter of kinetics. The ideal glass is the glass in which the energy has the lowest possible value at 0 K, and hence is that in which the constraints on the configuration are realized to the maximum extent possible. It is of interest to decide on the temperature at which it would be reached during infinitely slow cooling of the equilibrated liquid state. This can be achieved in different ways, of which the most general is by analysis of the temperature dependence of the relaxation time or, alternatively and less satisfactorily, of the viscosity.

Supposing that the liquid relaxation times, and the viscosity, can be described by the Adam–Gibbs equation [44], and that the Adam–Gibbs (AG) equation can be equated to the Vogel–Fulcher–Tammann (VFT) equation, the ideal glass temperature (now usually designated T_K) can be obtained from data as follows:

(a) We have

$$\tau = \tau_0 \exp(B/[T - T_0]) \text{ (VFT equation)} \equiv \tau_0 \exp(DT_0/[T - T_0]). \quad (2)$$

After introduction of the glass transition temperature T_g , defined at a relaxation time 16 orders of magnitude longer than τ_0 , equation (2) can be converted to

$$T_g/T_0 = 1 + [D/\ln(10)] \log(\tau_g/\tau_0) = 1 + D/[16 \ln(10)] \quad (3a)$$

from relaxation times, and

$$T_g/T_0 = 1 + [D/\ln(10)] \log(\eta_g/\eta_0) = 1 + D/[17 \ln(10)] \quad (3b)$$

from viscosity, η , because $\log \eta_g = 17 \log \eta_0$ [14].

(b) The Adam–Gibbs equation expresses the relaxation time in terms of the amount of entropy introduced into the liquid by excitation above the ground-state temperature T_K , according to the expression

$$\tau = \tau_0 \exp(C/T S_c). \quad (4)$$

(c) Evaluation of S_c in equation (4) yields equation (2) if the heat capacity has a particular simple form, i.e. is hyperbolic in T , as often seems to be the case for molecular liquids [45, 46], and we assign $S_c = 0$ when $T = T_K$. This procedure identifies the ground-state

temperature of the Adam–Gibbs analysis with the T_0 of the Vogel–Fulcher–Tammann equation. Thus we can obtain T_K from transport data through T_g and the fragility.

The fragilities of glass-forming liquids have been quantified both by the parameter D , and by the slope m of the relaxation time (or viscosity) near T_g according to

$$m = d \log \tau / d \log [T_g / T]. \quad (5)$$

Both D - and m -values have been quoted in the chalcogenide glass literature [31], and they may be interconverted using the relations

$$m = 16 + 590/D \quad (\text{for relaxation times}) \quad (6a)$$

and

$$m = 17 + 590/D \quad (\text{for viscosities}). \quad (6b)$$

The values of T_g which are to be ‘corrected’ according to these relations are shown in figure 4 (full triangles). The values of D or m needed to obtain the ground-state temperatures are available from the study of viscosity in reference [31], and from the study of mechanical relaxation times in reference [36]. The data are also available in principle [15, 16] from the widths of the glass transition though these were not systematically measured in reference [31]. The widths of the transitions seen in figure 5 have been correlated with $\langle r \rangle$ in a subsequent paper [47], and their utility in this respect will be mentioned later in this paper. The D -values used to extract T_0 -estimates are taken from figure 2 of reference [31](a) and m -values for the same purpose are taken from figure 2 of reference [31](b). The results for the ideal glass transition temperature (based on the identity of T_0 and T_K , demonstrated most recently in [42]) are plotted in figure 4 versus the mean bond density $\langle r \rangle$. Some additional points based on the more appropriate relaxation time–temperature dependences [36] are included. The value of T_K for Se, which is obtained from purely calorimetric data [31], is included in figure 4. It will later be seen that a finite T_K (and likewise T_0) is probably an artifact of extrapolation of observables, but it remains a useful characterizing parameter irrespective of the behaviour below T_g (the latter can only be determined from theory).

2.2.3. Percolation at $\langle r \rangle = 2.4$. Figure 4 gives an impression of the effect of constraints, represented by $\langle r \rangle$, on the rigidification of the system which is quite different to that given by the normal glass transition temperature displayed in the same figure. Insofar as the ideal glass transition temperature shows a weak dependence on $\langle r \rangle$ up to the value 2.4, and thereafter a steep increase, it is more in accord with theoretical expectations. Of course it needs to be substantiated by more detailed relaxation time studies over a wider range of substances. Data needed to extend the present type of analysis seem to exist in the work of Senapati and co-workers [32] for the system Ge–Sb–Se, and of Nemilov [33] for the system Ge–Se.

It is instructive to examine Nemilov’s viscosity data, because of their extension far above T_g . They are shown in figure 5 using the T_g -scaled viscosity plot which has become familiar in recent years. The $F_{1/2}$ -fragility [19] is assessed for the composition of maximum strength $r \geq 2.45$, using the construction shown, and found to be 0.24, comparable with that of sodium disilicate. The data for pure Se show an anomaly. The $F_{1/2}$ -fragility assessed at $\log(\eta/p) = 4.5$ is much smaller (0.52) than that obtained from the steepness index $m = 79$ (see figure 5), via the relation

$$F_{1/2} = [m - 16]/[m + 16] = 0.66. \quad (7)$$

This is unusual, and implies a serious breakdown in the VFT equation for this substance. This is probably due to a ring-chain contribution to $d\eta/dT$ at temperatures near T_g —which will not be discussed further here.

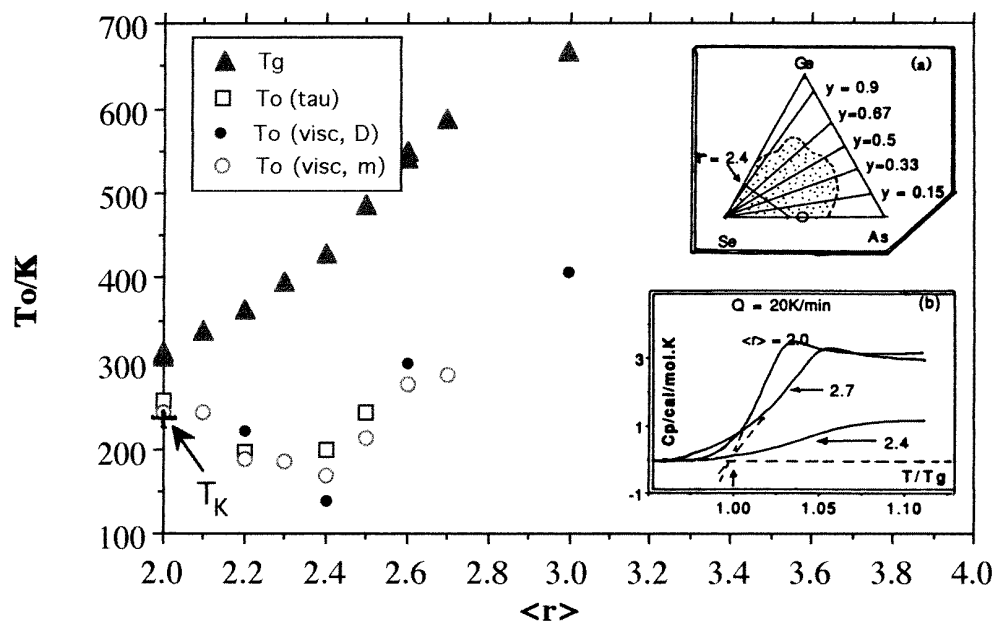


Figure 4. Comparison of the ideal glass transition temperatures $T_{0,i}$ with laboratory glass transition temperatures T_g for Ge-As-Se alloys along the join with $[Ge]/[As] = 1$ (i.e. $Y = 0.5$, in inset (a)). The spread of values for viscosity temperatures T_0 between D - and m -based values indicates the uncertainty in fragility determination by these methods since the raw data are the same. The confirmation by the quite independent mechanical relaxation measurements is reassuring, and the special nature of the bond density 2.4 is clearly seen. For pure Se, an ideal temperature, T_K , is obtainable from purely thermodynamic data, and its value is indicated by the arrow. Inset (b) shows the form and magnitude of the heat capacity in excess of the glass (also Dulong and Petit) value above T_g . Note that the value of $C_{p,ex}$ for $r = 2.4$ corresponds closely with the Schottky anomaly value $0.9 \text{ cal K}^{-1}/(\text{g atom})$.

Instead we proceed to a theoretical description of the observations at the simplest possible level of statistical thermodynamics in order to show how an account of the observed differences between the experimental and ideal glass transition curves seen in figure 5 can be reduced to an account of the composition dependence of two parameters of familiar character.

2.2.4. The 'bond' model for the observed behaviour of Ge-Se liquids. To provide a first-approximation account of the way the observed behaviour obscures the fundamental accord with rigidity theory, we turn to the 'bond lattice' description of the thermodynamic excitation of a system of bonded particles. This approach is in fact more appropriate for the covalently bonded chalcogenides than for almost any other type of glassy system. A previous case for which the equations of this treatment seem appropriate, and indeed provide an adequate account of the observations, is the partly covalent system $ZnCl_2$ [48].

In the bond lattice approach [49], the system of strongly bonded particles is transposed to its 'bond lattice' in which the elements of the lattice can justifiably be considered as weakly interacting and can therefore be treated, in the first approximation, as being independently excitable. The number of bonds in the bond lattice of a chalcogenide ideal glass depends on composition: $2N$ for Se, $3N$ for GeSe, where N is the number of atoms.

In the rigidity arguments for chalcogenide systems, bond angles are considered equally as constraining as bonds, and we will maintain this simplification in our treatment here.

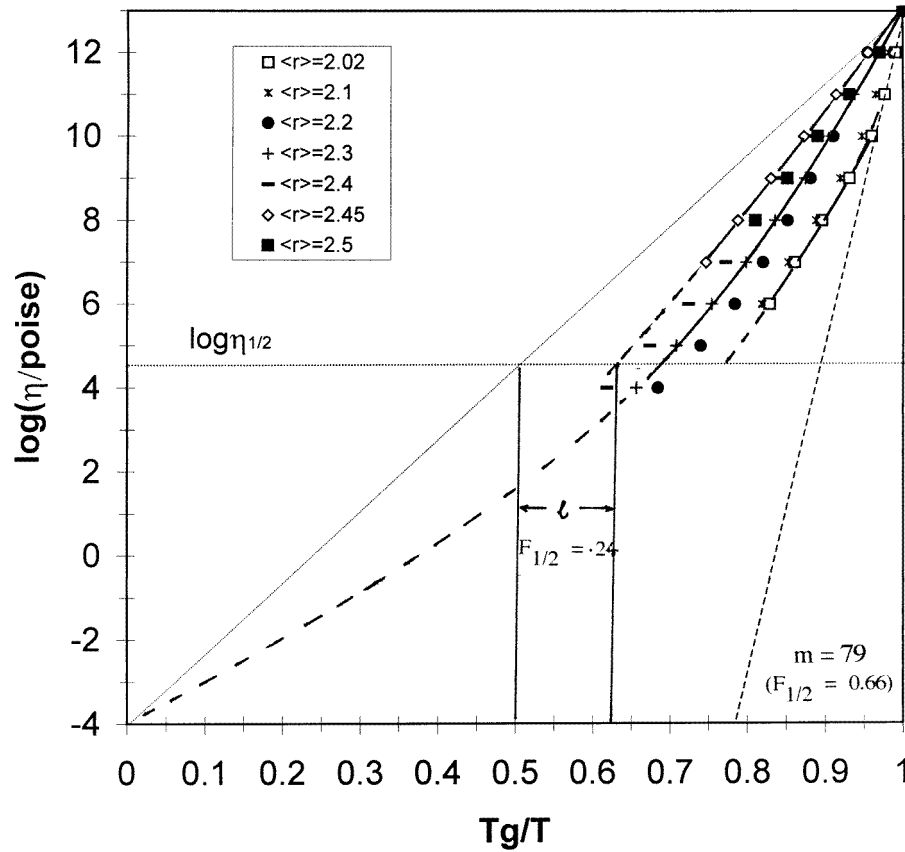


Figure 5. A T_g -scaled Arrhenius plot of viscosity data for Ge + Se melts, showing the wide range of fragilities exhibited as the bond density is changed. The graph shows the definition of the 'steepness index' m and the preferred fragility metric, $F_{1/2}$ [8] ($F_{1/2} = 2l$). Pure Se shows m - and $F_{1/2}$ -values which are not consistent, evidently due to special structures near T_g .

It is, however, a simple matter to introduce states of different excitation energy and to describe the multistate excitation. However, this introduces extra parameters without changing the qualitative behaviour in important ways [34] unless the constraints have very different excitation energies or entropies.

A system with intact constraints (bonds) clearly has a lower enthalpy per mole of constrained particles than one with the constraints broken. Focusing on the constraints themselves, we assign an enthalpy of constraint breaking of ΔH^* . Then the distribution of constraints across the 'constraint quasi-lattice' will vary with temperature and pressure according to the usual two-state thermodynamic relations known for Schottky anomalies in low-temperature magnetic systems and since applied to various physical systems by many workers [51–54].

In the systems described by Schottky, which give rise to smeared-out heat capacity bumps known as Schottky anomalies, the flipping of a spin causes no entropy change other than that associated with the distribution of different spins among the N magnetic species in the structure. This seems to be almost the same situation as that for an optimally constrained bond lattice, as will be seen. However, in under-constrained systems (and also, it seems, in

over-constrained systems) the lifting of a single constraint may give rise to more alternative configurations or excited phonons than are indicated by the standard distribution across the constraint lattice. This can be accommodated by including an entropy-of-excitation term $S_2 - S_1 (= \Delta S^*)$. ΔS^* may be due to a local structure degeneracy, y , introduced on bond breaking, $\Delta S^* = R \ln y$, or may be vibrational in character, arising because the excitation is accompanied by a decrease in average vibration frequency for the quasi-lattice region containing the ‘defect’ ($\Delta S_{vib} = R \ln(v_1/v_2)$).

In view of the importance of this issue, which we will see is at the core of fragility, we must note that in a related case, the excitation of interstitial defects in crystal lattices, the generation of low-frequency vibrational modes accompanies defect formation, and provides a strong entropic drive to increase the defect population [54]. We suspect that a similar phenomenon is the source of the well known but poorly understood quasi-elastic neutron scattering intensity build-up in glass formers above T_g [41]. It is, in this case, no surprise that this intensity build-up is most striking in the case of fragile liquids, since this implies a larger ΔS^* , which we will see controls fragility, for such cases.

The formal two-state thermodynamic development follows as

$$\text{state I} \leftrightarrow \text{state II}$$

that is

$$[\text{bond and angle constraints intact}] \leftrightarrow [\text{broken constraints}]$$

denoted as

$$A \leftrightarrow B$$

for which, in a first approximation (ideal mixing, or independent bond-breaking), the equilibrium constant K_{eq} is given by

$$K_{eq} = [A]/[B] = X_B/(1 - X_B) \quad (8)$$

and

$$\Delta G^* = \Delta H^* - T \Delta S^* = RT \ln K_{eq} \quad (9)$$

where ΔH^* is the enthalpy per mole of constraint breaking (elementary excitation) and ΔS^* (discussed above) is the entropy change *in excess of* the entropy increase due to distribution of broken bonds across the ‘bond lattice’.

From equation (9) the mole fraction of broken bonds is found to be

$$X_B = [1 + \exp(\Delta H^* - T \Delta S^*)/RT]^{-1} \quad (10)$$

and the associated heat capacity is

$$C_p = (\partial H / \partial T)_p = R(\Delta H^* / RT)^2 X_B(1 - X_B). \quad (11)$$

This heat capacity is a dome with its onset commencing at a temperature determined by the molar enthalpy increment per constraint break, ΔH^* . When the system is non-optimally constrained, $\langle r \rangle \neq 2.4$, the extra entropy term ΔS^* causes a more rapid increase and then the heat capacity has a maximum value which is determined by the magnitude of ΔS^* . The general behaviour for different ΔH^* , ΔS^* combinations may be seen in figures 6 and 7. The ability to fit the data on liquid ZnCl_2 , which is an intermediate-fragility liquid, is indicated in the figure. The value of ΔS^* required is quite small. Note that the two distinct sources of ΔS^* discussed above imply distinct vibrational and configurational contributions to the observed jump in C_p at the glass transition, as analysed by Goldstein long ago [40].

For the case of Ge-As-Se at the bond density 2.4, the maximum heat capacity rise is only a little over $1 \text{ cal mol}^{-1} \text{ K}^{-1}$ (see figure 4, inset). Since at this composition there are

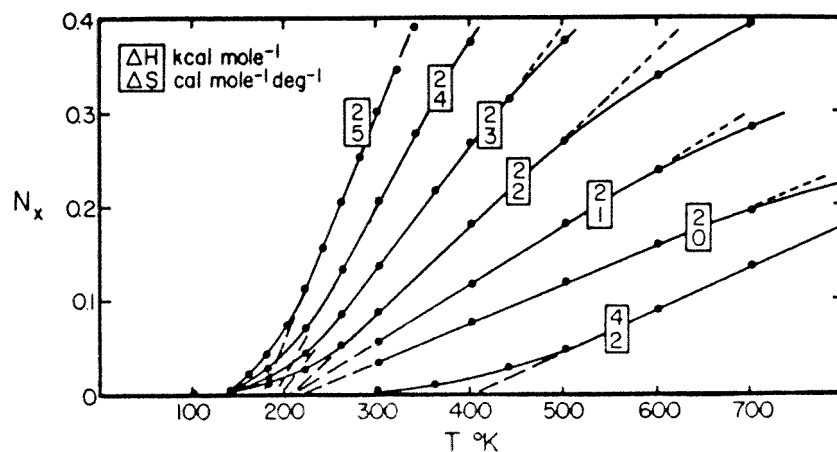


Figure 6. The fraction of constraints broken at different temperatures for the equation (10) parameter sets indicated in boxes alongside the plots. Note that extrapolation of the linear portions to low temperatures defines an operational ground-state temperature, a Kauzmann temperature, which is seen to be determined almost entirely by the value of ΔH . The rate of excitation above the T_K , which determines the thermodynamic fragility (and also the relaxational fragility—see below), is however determined by the value of ΔS . (From reference [24], by permission.)

1.2 moles of bonds per mole of atoms, the value of ΔC_p measured is close to the value for the Schottky anomaly at its broad maximum—namely, $0.9 \text{ cal K}^{-1} \text{ mol}^{-1}$ of excitations (here broken bonds). This corresponds to the case where $\Delta S^* = 0$. Conversely (figure 7), high heat capacity jumps at T_g must be a direct consequence of a large constraint-breaking entropy increment, ΔS^* of equation (9).

2.2.5. Relaxation in the liquid state. In references [24] and [49] it was argued that the probability of a rearrangement of atoms, such as is needed for a fundamental diffusive event or flow event to occur, must depend on the presence of a critical fluctuation in the local concentration of broken constraints. Invoking the Lagrangian-undetermined-multipliers treatment of constrained maxima [55], this probability is found to be an exponential function of the fraction of broken constraints at each temperature. This gives rise to a three-parameter expression for the temperature dependence of the relaxation probability $W(T)$:

$$W(T) \sim \exp(f^*/X_B(T)) \quad (12)$$

where f^* is a critical local broken-constraint fraction and X_B is the overall broken constraint fraction, determined by the two parameters ΔH^* and ΔS^* of equation (9). X_B has been plotted in figure 6. Expression (12), which becomes a transcendental equation with parameters ΔH^* and ΔS^* when X_B is substituted for with equation (10), is indistinguishable in fitting ability from the two-parameter exponent of the VFT equation, equation (2). In fact, in the range of T near T_g , X_B is linear in T , and hence equation (11) becomes the VFT equation. The VFT parameter T_0 is the extrapolated intersection of the equation (10) function with the T -axis at $X_B = 0$, and the VFT parameter B is the inverse of the slope dX_B/dT modified by the parameter f^* , which is between zero and unity.

For $f^* = 1$, the parameter D of equation (2), which describes the ‘strength’ of the liquid, is found to be determined entirely by the magnitude of the ΔS^* parameter, and to maximize when ΔS^* is zero as in the Schottky anomaly. This is shown elsewhere [24, 49] where B is

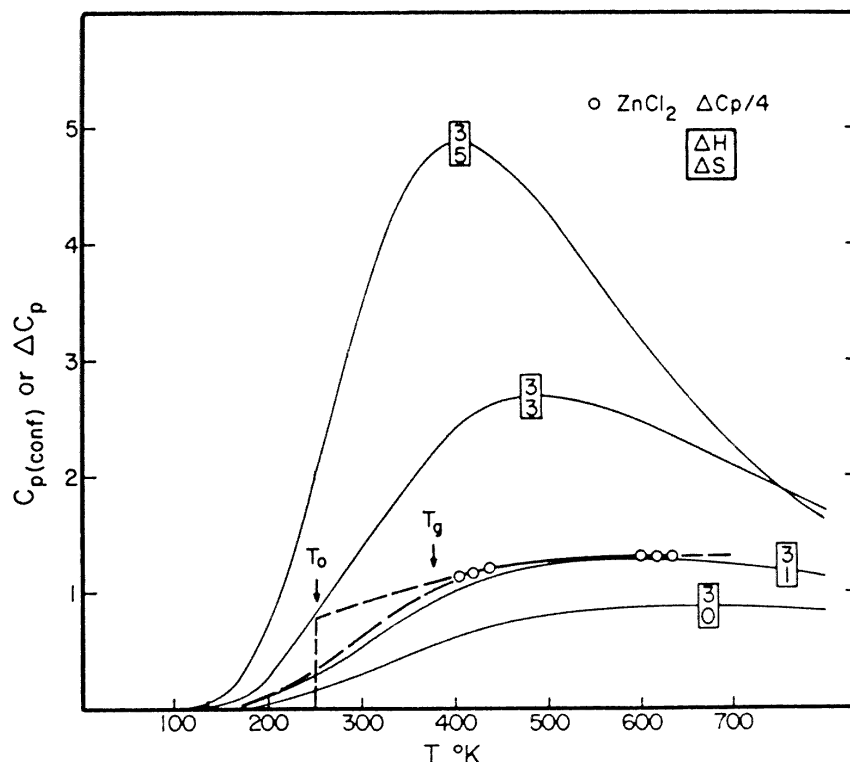


Figure 7. Variations of the heat capacity with temperature according to equation (11) for the parameter sets indicated alongside the curves. Comparison is made with the case of ZnCl_2 for data obtained near the glass transition temperature and above the melting point, and the deviation of the theoretical curve from that assumed in calculating the Kauzmann temperature for this substance [29] is noted. The assessment assumes four breakable bonds per mole of ZnCl_2 . (Adapted from reference [1], by permission.)

seen to be a linear function of T_0 ; hence $D = B/T_0$ as in equation (2). T_0 , on the other hand, is determined almost entirely by the ΔH^* parameter, as shown by the linear extrapolations to $X_B = 0$ in figure 6. This was demonstrated [49] before the ‘strong/fragile’ classification of liquids was expressly formulated and has not been discussed in relation to fragility before. According to this line of thought, and figure 6(b) of reference [49](b), the maximum value of D would be 11 if f^* had the value of unity. This is far smaller than is observed in practice, where values up to 83, close to the strong-liquid extreme, have been observed for the Ge–As–Se system [31]. To account for this, values of f^* much smaller than unity, namely, $\simeq 0.13$, are needed. Certainly it is reasonable for rearrangements to be possible with local broken-bond fractions smaller than unity. Discussion of such details is deferred to a future paper.

Two-state treatments of physical phenomena fall at the lowest level of sophistication in statistical thermodynamics, and we would not introduce them here were it not for two features that we think provide considerable insight into the physics of fragile liquids and their current interpretation in terms of ‘energy landscapes’.

The first is the obvious one that the two-state analysis provides a one-parameter (ΔS^*) interpretation of thermodynamic fragility of chalcogenide liquids, and a two-parameter (ΔS^* , f^*) description of relaxation fragility. This in turn should encourage further exp-

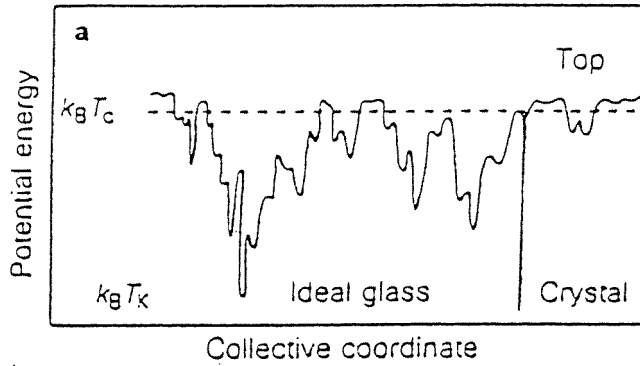


Figure 8. (a) The 2D representation of the energy ‘landscape’ for a system of interacting particles, indicating the relation between crystal, liquid, and ‘ideal-glass’ states. This suggests that the ‘top of the landscape’ falls near the mode-coupling critical temperature T_c . (b) The relation between the portion of the energy landscape visited by the system most frequently and the temperature of the system, according to recent MD computer simulation inherent-structure studies [19]. To obtain the ergodic behaviour at lower temperatures, the profile has been extrapolated linearly to the temperature T_K according to the relation $T_c/T_K = 1.6$ observed for a variety of fragile liquids in laboratory studies [20]. T_c , according to the MD studies of reference [39], is 0.435 in panel (b) units. The ‘width’ of the profile defined by the linear extrapolation of the steep part of the profile to the ground state and to the ‘top’ is indicated by vertical dashed lines. (c) The equation (9) excitation profile for parameters (in the box) and T -units which approximately match the width of the mixed-LJ-system profile of panel (b). For equation (9), the ‘top’ of the excitation profile is only reached at $T = \infty$. The general similarity of the panel (b) and panel (c) excitation profiles can be used to advantage to simplify the description of liquid properties which are necessarily complex in multidimensional energy landscape terminology. Note the ergodic behaviour near T_K . The gradient of the excitation profile gives a measure of the density of configurational states for the liquid.

experimental and theoretical efforts to understand properly the origin of the extra degeneracy introduced when local excitations (constraint breaks) occur in liquids.

The second is more provocative and relates to the light that this analysis sheds on the excitation profile discussed in section 1 (in relation to the ‘energy landscape approach’ description of complex systems).

3. Comparison of the excitation profile from MD computer simulation studies of the mixed LJ system with profiles from the bond model

In section 1, figure 1, the excitation profile was depicted as a plot of the energy that the (mixed LJ) system, equilibrated at temperature T , retained when the non-configurational energy was suddenly removed by a procedure which ensured that the system was trapped directly in the ‘landscape’ minimum above which it was located at the moment of quench. Repeat runs ensure that, even for the small system under study, the energy of this minimum is confined to a small band for each temperature below the value ~ 1.0 in system units. The understanding is that this is the value of energy E to which the system is driven at temperature T by the TS -product in the Helmholtz free energy $A = E - TS$, where S is given by $k_B \ln W$, W being largely, but not wholly, the number of landscape minima to which the system has access. The other component of W will lie within the vibrational manifold, as was discussed already in section 2.2.4 in relation to the nature of ΔS^* .

In terms of the bond model, the system is driven to a given state of configurational excitation

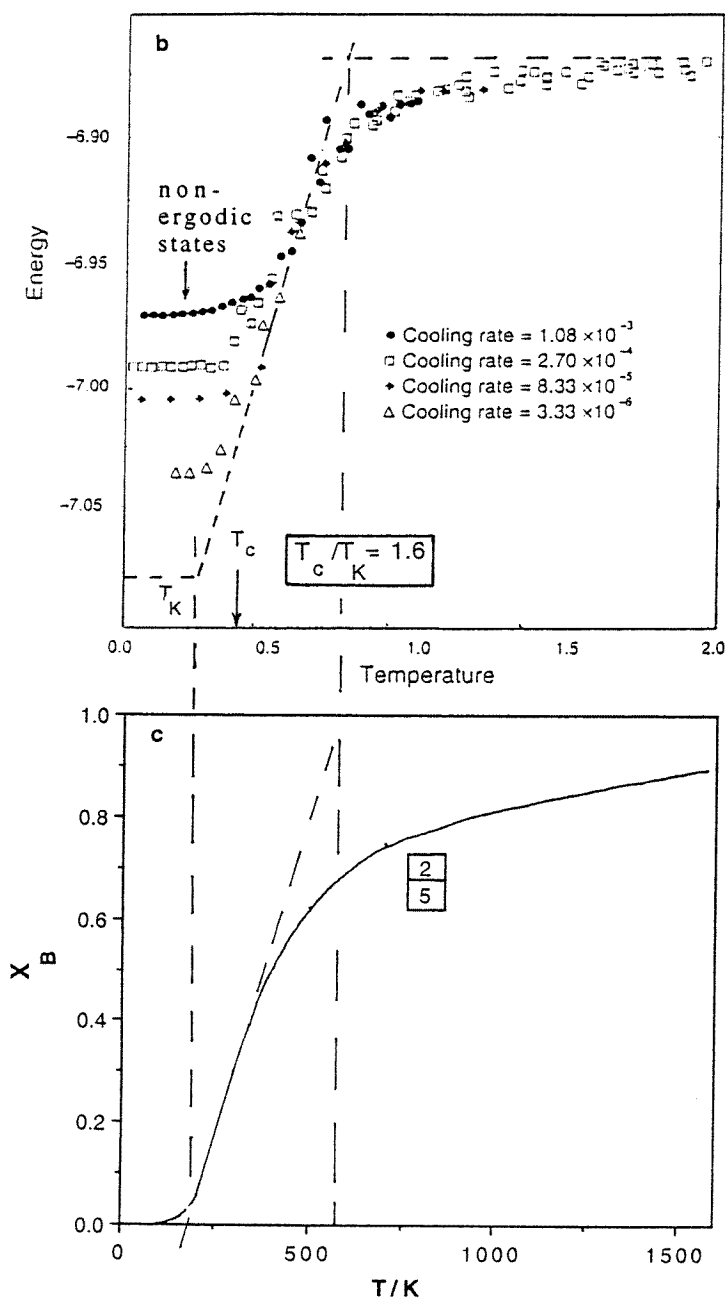


Figure 8. (Continued)

(X_B) by exactly the same factors, and so the excitation profile should be given directly by the equation for X_B . The configurational energy for an isochoric system would be simply the $X_B \Delta E^*$ product. We can therefore make a direct comparison of the profile obtained by configuration-space considerations and by simple elementary-excitations arguments.

3.1. Excitation profiles and densities of configuron states

The relation between the excitation profile obtained from simulations of mixed LJ systems (figure 1) and that calculated using equation (10), with parameters chosen to give the same ‘reduced width’ as for the LJ system, is shown in figure 8. The reduced width is the ratio of temperatures obtained by extension of the steep linear part of the excitation profile to the ‘top of the landscape’ of panel 2 on the one hand and to the ground-state level on the other (see the vertical dashed lines in panels (b) and (c) which delineate the ‘widths’) [56]. The top of the landscape in panel (c) is the high-temperature limit of X_B , which is $1/[1 + \exp(-\Delta S/R)]$ whenever ΔS^* differs from 0, or 0.92 in the case of figure 8(c).

The resemblance of the excitation profiles for the mixed LJ system (panel (b)), and the simple two-state model (panel (c)) is quite impressive and, we think, instructive insofar as one is obtained from a configuration-space representation of the system thermodynamics and the other is based on a real-space representation. The implication is that any instantaneous collection of bond lattice excitations represents a configuration-space minimum, and can be ‘frozen in’ for evaluation by conjugate gradient quenching. This is of course the starting premise in any two-state treatment—namely that the vibrational excitations of the particle lattice are separable from the configurational excitations of the bond lattice. The separability depends on the same difference in relaxation times which makes quenching in of a configuration a possibility.

The equation (3) profile approaches the fully excited limit more gradually than does the LJ system. There is more of a ‘shelf’ before the plunge to the configurational ground state. This difference may be associated with the constant value assumed for ΔS^* . If an important part of ΔS^* comes from the generation of low-frequency modes in the vibrational density of states (being revealed as the quasi-elastic scattering intensity build-up in neutron scattering studies), then it is not unreasonable to suppose that the new vibrational modes excited should become *lower* in frequency as the structure becomes looser, thus accelerating the drive to full excitation [57] as seen in figure 8(b).

Note that we have had to invoke a rather large excitation entropy in order to match the width of the mixed-LJ-system profile defined as in panel (b) of figure 8. The value of $\Delta C_{p,max}$ corresponding to this value of ΔS^* is (figure 7) $4.8 \text{ cal mol}^{-1} \text{ K}^{-1}$ which corresponds closely with the mixed-LJ-system value for ΔC_p at the MD glass transition, namely $4.3 \text{ cal mol}^{-1} \text{ K}^{-1}$ [58] if there is only one constraint per particle. The corresponding D -value ($D = B/T_0$), according to figure 6(b) of reference [49](b), should be approximately 3 for $f^* = 1.0$, compared with $D = 8$ for Se, the most fragile liquid in the Ge–As–Se system. The value 3 is characteristic of a very fragile liquid [42] as would be expected at first sight for a mixed LJ system. However, we have seen in section 2.1 that a mixed LJ system is probably only moderately fragile and a value of D more like 10 should be expected. Thus again a value of f^* well below 0.5 is indicated. If the profile of figure 1 and figure 8(b) is that of a moderately fragile liquid, then we must ask what is expected for the profiles of very fragile liquids on the one hand, and very strong liquids on the other. Here the bond model provides simple answers if independent bonds are assumed and interesting answers if non-random bonding is introduced. The latter case is considered in a final section.

In more fragile systems, as discussed earlier with respect to figure 6, the system is driven to full excitation more quickly by the presence of larger excitation entropy values. Also the inflection point in the profile will occur at higher excitation fractions. If the excitation entropy ΔS^* is configurational rather than vibrational in origin, then the excitation profile can be taken as a reflection of the density of configurational states, which will then be obtained from the gradient of the profile. The density of states will be bell shaped, and narrow in

proportion to the fragility. The peak value will occur at the profile inflection temperature. If ΔS^* is largely vibrational in nature, then the density of states is less important than the excitation profile. Stronger liquids will have excitation profiles widely spread in temperature, and will pass the melting points and even their boiling points before they reach the tops of their landscapes. Thus the intermediate liquid ZnCl_2 , which shows the presence of the predicted C_p -maximum (figure 6), will melt while the landscape is only partly excited. Accordingly, the entropy of fusion is less than R entropy units per mole of heavy atoms (the measured value is $0.66 R/(\text{g atom})$). Likewise SiO_2 , which melts to give the strongest liquid known (except for glassy water [15]), melts with far fewer than R entropy units per mole of heavy atoms (the measured value is $0.37 R/(\text{g atom})$).

In the fully covalent systems, this broadest density of states is realized for compositions with optimized bond densities, for which the excitation entropy approaches zero, as we have seen earlier.

It is worthwhile to compare these observations with those of Speedy for hard-sphere systems. Speedy [21, 63–65] has argued plausibly, on the basis of simulations for a variety of hard-sphere systems, that the density of states (alternate-packing schemes) is most probably Gaussian (and in this respect a little different from that of our simple model). In one of these systems, the ‘tetraivalent hard-sphere system’ [21], constraints were applied. The Gaussian for this case was much broader than for the simple hard-sphere system, so the tetraivalent system is a ‘stronger’ liquid in our terminology—consistent with what we see in the constraint lattice model, and in the corresponding laboratory chalcogenide glasses, as constraints are optimized. However, Speedy [65] examined the effect of the constrained coordination number on the properties of the hard-sphere system without finding any behaviour reminiscent of that shown in figure 3. The origin of such differences between hard-sphere fluids and the model chalcogenide systems may be due to the absence of angular constraints in the former. A systematic study of these factors should do much to enhance our understanding of fragility in the liquid state.

3.2. Excitation profiles and ‘crossover’ phenomena

The position of the mode-coupling-theory T_c on the profile of the mixed LJ system, figure 8(b), is of interest. It is more than half-way down to the ground-state energy, and close to the inflection point of equation (9) seen in figure 8(c). This is consistent with the observations of Fischer [53] who fitted equations based on the two-state model to the experimental data for several molecular liquids for which T_c had been determined by other workers. (It is below this energy that over half of the many orders-of-magnitude changes of the relaxation time occur *en route* to the glass transition.)

A number of studies [8, 19, 22, 59, 60] have identified the temperature T_c with the temperature at which there is some crossover in the temperature dependence of relaxation times, and now [19], some breakdown in the agreement of Vogel–Fulcher and Adam–Gibbs descriptions which fit the low-temperature relaxation data so well for most liquids [19]. The departure from near-linearity in temperature of the function X_B , which is the denominator of the relaxation probability expression, provides (via equation (12)) a rather direct explanation for the failure of the Vogel–Fulcher equation.

From the figure 8 comparison, we can go on to describe, at least qualitatively, the energy landscape excitation profiles for chalcogenide liquids with different values of $\langle r \rangle$ using the fragilities measured in reference [31], and the equation (9) ‘excitation profiles’ for the associated constraint-breaking parameters ΔH^* and ΔS^* . This analysis will be presented in

more detail when a study of the simple two-component system Ge–Se, currently in progress, has been completed [61].

3.3. Non-random bonding and liquid–liquid phase transitions

Of additional interest in the chalcogenide systems is the existence of a maximum T_g -value as Ge content increases and the system becomes severely over-constrained. The existence of a general maximum can be deduced from the knowledge that the diffusivity of crystalline Ge exceeds that characteristic of a substance at its glass transition ($10^{-22} \text{ m}^2 \text{ s}^{-1}$) at 550 K [66], so amorphous Ge must presumably have a T_g -value no higher than 550 K. (This is close to its observed recrystallization temperature.) The maximum has been directly observed in the case of the Ge–Se system [39, 67] and can be associated with an effective reduction of the Ge oxidation state towards +2 (GeSe). A T_g of 550 K is reached at 35% Ge in the binary system and should be found in any cut through the ternary system at comparable Ge fractions. Although it has not been reported to date, this would probably be followed by the splitting out of a pure liquid Ge phase with about the same T_g -value. In this domain the independent constraint-breaking assumption made in the two-state treatment we have given must break down, and interesting analogies with the landscape interpretations of polyamorphism [68] will present themselves.

In the maximally over-constrained cases, Ge and Si, first-order liquid–liquid phase transitions are believed to occur [69]. They have been observed in detail in computer simulation studies of Si [70]. These can be explained if the bond-breaking is taken to be cooperative in the sense of regular solutions. Then a composition with a critical point will exist, and beyond that composition the sigmoid excitation profile of figure 8(c) will become an ‘S’-shaped curve—meaning that two distinct states of excitation can coexist at the same temperature. These will be the high- and low-density phases of liquid Si (and Ge) identified by laser fusion [69] and computer simulation [70] studies.

Acknowledgments

This was carried out under the auspices of the NSF under Solid State Chemistry grant No DMR 9614531. The author has benefited from helpful discussions with Burkhard Geil and Robin Speedy, and is indebted to Paul Madden for drawing our attention to the low-frequency lattice vibrations accompanying interstitial excitations in crystals and the possible analogy to bond lattice excitations in the present model. Pierre Lucas is thanked for preparing figure 5 from the data of Nemilov [33].

References

- [1] Sastry S, Debenedetti P G and Stillinger F H 1998 *Nature* **393** 554
- [2] Stillinger F H and Weber T A 1984 *Science* **225** 983
- [3] Angell C A, Clarke J H R and Woodcock L V 1981 *Adv. Chem. Phys.* **48** 397
- [4] Jonsson H and Andersen H C 1988 *Phys. Rev. Lett.* **60** 2295
- [5] Götze W 1989 *Liquids, Freezing, and the Glass Transition (Les Houches)* ed J-P Hansen and D Levesque (Amsterdam: North-Holland)
- [6] Kob W and Andersen H C 1995 *Phys. Rev. E* **51** 4626
- [7] Kauzmann W 1948 *Chem. Rev.* **43** 219
- [8] Angell C A 1967 *Complex Behaviour of Glassy Systems* ed M Rubi (Berlin: Springer)
- [9] Angell C A 1997 *Proc. Int. Enrico Fermi School of Physics (Course CXXXIV)* ed F Mallamace and H E Stanley (Amsterdam: IOS Press)
- [10] Richards B E, Velikov V and Angell C A 1999 to be published

- [11] Choi Y 1984 *MSc Thesis* Purdue University, West Lafayette, IN
- [12] *Handbook of Chemistry and Physics* 1995 76th edn (Boca Raton, FL: Chemical Rubber Company Press) pp 6–245
- [13] Laughlin W T and Uhlmann D R 1972 *J. Phys. Chem.* **76** 2317
- [14] Angell C A and Sichina W *Ann. NY Acad. Sci.* **279** 53
Angell C A 1985 *Relaxations in Complex Systems* ed K Ngai and G B Wright (Springfield, VA: National Technical Information Service, US Department of Commerce)
- [15] Ito K, Moynihan C T and Angell C A 1999 *Nature* at press
Ito K, Angell C A and Moynihan C T 1999 to be published
- [16] Moynihan C T 1993 *J. Am. Ceram. Soc.* **76** 1081
- [17] Wu L 1991 *Chem. Rev.* **B 43** 9906
- [18] Baranek M, Breslin M and Berberian J G 1994 *J. Non-Cryst. Solids* **172–174** 223
- [19] Richert R and Angell C A 1998 *J. Chem. Phys.* **108** 9016
- [20] Angell C A and Tucker J C 1999 to be published
- [21] Speedy R J and Debenedetti P G 1995 *Mol. Phys.* **86** 1375
- [22] Rössler E and Sokolov A P 1996 *Chem. Geol.* **128** 143
- [23] Stickel F, Fischer E and Richert R 1996 *J. Chem. Phys.* **104** 2043
- [24] Angell C A and Rao K J 1972 *J. Chem. Phys.* **57** 470
- [25] Thorpe M F 1983 *J. Non-Cryst. Solids* **57** 355
Philipps J C and Thorpe M F 1985 *Solid State Commun.* **53** 699
- [26] Philipps J C 1979 *J. Non-Cryst. Solids* **34** 153
- [27] Weber P J and Savage J A 1976 *J. Non-Cryst. Solids* **20** 271
- [28] He H and Thorpe M F 1985 *Phys. Rev. Lett.* **54** 2107
- [29] Thorpe M F 1997 *Amorphous Insulators and Semiconductors (NATO-ASI Series)* ed M F Thorpe and M I Mitkova (New York: Plenum)
- [30] Halfpap B L and Lindsay S M 1986 *Phys. Rev. Lett.* **57** 847
- [31] (a) Tatsumisago M, Halfpap B L, Green J L, Lindsay S M and Angell C A 1990 *Phys. Rev. Lett.* **64** 1549
(b) Böhmer R and Angell C A 1992 *Phys. Rev. B* **45** 10 091
- [32] Senapati V and Varshneya A K 1995 *J. Non-Cryst. Solids* **185** 289
Varshneya A K, Sreeram A N and Swiler D R 1993 *Phys. Chem. Glasses* **34** 179
- [33] Nemilov S V 1964 *Zh. Prikl. Khim.* **37** 1020
- [34] Tanaka K 1986 *Solid State Commun.* **60** 295
- [35] Asokan S and Gopal E S R 1986 *Rev. Solid State Sci.* **3** 273
- [36] (a) Boolchand P, Bresser W, Zhang M, Wu Y, Wells J and Enzweiler R N 1995 *J. Non-Cryst. Solids* **182** 143
(b) Boolchand P and Thorpe M F 1994 *Phys. Rev. B* **50** 10 366
(c) Boolchand P, Zhang M and Goodman B 1996 *Phys. Rev. B* **53** 11 488
- [37] Halfpap B 1990 *PhD Thesis* Arizona State University, Tempe
Halfpap B, Lindsay S M and Angell C A 1999 to be published
- [38] Feltz A 1993 *Amorphous Inorganic Materials and Glasses* (Weinheim: VCH)
- [39] Angell C A 1999 *Rigidity: Theory and Applications* ed M F Thorpe and P M Duxbury (New York: Plenum) at press
- [40] Goldstein M 1969 *J. Chem. Phys.* **51** 3728
Goldstein M 1976 *J. Phys. Chem.* **64** 4767
- [41] Articles in *Science* 1995 **267** 1924 (special issue)
- [42] Angell C A 1997 *J. Res. NIST* **102** 171
- [43] (a) Turnbull D 1969 *Contemp. Phys.* **10** 473
(b) Angell C A 1968 *J. Am. Ceram. Soc.* **51** 117
- [44] Adam G and Gibbs J H 1965 *J. Chem. Phys.* **43** 139
- [45] Privalko Y 1980 *J. Phys. Chem.* **84** 3307
- [46] Alba C, Busse L E and Angell C A 1990 *J. Chem. Phys.* **92** 617
- [47] Lucas J, Hong Li Ma, Zhang X H, Senapati H, Böhmer R and Angell C A 1992 *J. Solid State Chem.* **96** 181
- [48] Angell C A, Williams E W, Rao K J and Tucker J C 1977 *J. Phys. Chem.* **81** 238
- [49] (a) Angell C A 1971 *J. Phys. Chem.* **75** 3698
(b) Angell C A and Rao K J 1972 *J. Chem. Phys.* **57** 470
(c) Rao K J and Mohan R 1980 *J. Phys. Chem.* **84** 1917
- [50] Macedo P B, Capps W and Litovitz T A 1966 *J. Chem. Phys.* **44** 3357
- [51] Perez J 1985 *J. Physique Coll.* **46** C10 427
- [52] Kieffer J, Masnik J E, Nickolayev O and Bass J D 1998 *Phys. Rev. B* **58** 694

- [53] Wang C H and Fischer E W 1996 *J. Chem. Phys.* **105** 7316
Fischer E W 1999 *Preprint*
- [54] Granato A V 1992 *Phys. Rev. Lett.* **68** 974
Granato A V 1994 *J. Phys. Chem. Solids* **55** 931
- [55] (a) Cohen M H and Turnbull D 1959 *J. Chem. Phys.* **31** 1164
(b) Van Damme H and Fripiat J J 1978 *J. Chem. Phys.* **62** 3365
- [56] We note again [30] how the bond lattice treatment in the ‘independent-bond’ approximation denies the existence of a finite Kauzmann temperature, though it shows how an operationally defined ground-state temperature (which would be the T_0 of equation (2)) is obtained by a short extrapolation of the excitation profile. The transcendental equation, equation (11), fits transport and relaxation time data as well as does equation (2) [42] without requiring a finite ground-state temperature. However, it was shown in reference [30] that the glass transition phenomenon for fragile liquids is significantly sharper than can be accounted for by equation (10), and it is possible that cooperative effects, neglected in the zeroth-order model, may produce a genuine singularity in principle, though there is as yet no evidence for it. The possibilities are illustrated in reference [43].
- [57] Harrowell P and Angell C A 1999 to be published
- [58] Vollmayr K, Kob W and Binder K 1996 *Phys. Rev. B* **54** 15 808
- [59] Rössler E 1990 *Phys. Rev. Lett.* **65** 1595
- [60] Hansen C, Stickel F, Berger T, Richert R and Fischer E W 1997 *J. Chem. Phys.* **107** 22
- [61] Lucas P and Angell C A 1999 to be published
- [62] Sciortino F, Sastry S and Tartaglia P 1999 *Preprint*
- [63] Speedy R J 1998 *J. Phys.: Condens. Matter* **10** 4185
- [64] Speedy R J 1998 *Mol. Phys.* **95** 169–78
- [65] Speedy R J, private communication
- [66] Coffa S, Poate J M and Jacobson D C 1992 *Phys. Rev. B* **45** 8355
- [67] Feltz A and Lippmann F J 1973 *Z. Anorg. Allg. Chem.* **398** 157
- [68] Angell C A 1995 *Proc. Natl Acad. Sci. USA* **92** 6675
- [69] Thompson M O, Galvin G J, Mayer J W, Peercy P S, Poate J M, Jacobson D C, Cullis A G and Chew N G 1984 *Phys. Rev. Lett.* **52** 2360
- [70] Angell C A, Borick S and Grabow M 1996 *J. Non-Cryst. Solids* **205–207** 463